J. Fluid Mech. (1990), *vol.* 215, *pp.* 457–480
Printed in Great Britain

On the hydraulics of Boussinesq and non-Boussinesq two-layer flows

By GREGORY A. LAWRENCE
Department of Civil Engineering, University of British Columbia, Vancouver, BC, Canada, V6T 1W5

(Received 5 September 1986 and in revised form 9 November 1989)

Exact expressions for the internal and external Froude numbers for two-layer flows are derived from the celerities of infinitesimal long internal and external waves, without recourse to the Boussinesq approximation. These expressions are functions of the relative density difference between the layers; the relative thickness of the layers; and the stability Froude number, which can be regarded as an inverse bulk Richardson number. A fourth Froude number, the composite Froude number, has been most often used in previous studies. However, the usefulness of the composite Froude number is shown to diminish as the stability Froude number increases. The potential confusion associated with having four Froude numbers of importance has been alleviated by deriving an equation interrelating them. This equation facilitates a comprehensive understanding of the hydraulics of two-layer flows.

It is demonstrated that in substantial portions of some flows (both Boussinesq and non-Boussinesq exchange flow through a contraction are presented as examples), the stability Froude number exceeds a critical value. In this case hydraulic analysis yields imaginary phase speeds corresponding to the instability of long internal waves. Various implications of this result are discussed.

1. Introduction

Many flows of oceanographic, meteorological, and engineering importance can be modelled as homogeneous layers of inviscid fluid subject to a hydrostatic pressure distribution. The resulting one-dimensional (hydraulic) equations are used extensively in the study of single-layer, open channel flows, see Henderson (1966). The extension to multi-layer flows has been pursued since the early 1950s in studies concerned with the intrusion of salt water into estuaries and rivers (Stommel & Farmer 1953; Schijf & Schönfeld 1953), and with the flow of air over mountains (Benton 1954; Long 1954). More recently, interest in the hydraulics of layered flows has grown rapidly, resulting in the development of a general formulation by Houghton & Isaacson (1970), Baines (1984), and Armi (1986). An impressive recent application is a model of the exchange of Mediterranean and Atlantic water through the Strait of Gibraltar by Armi & Farmer (1986, 1989) and Farmer & Armi (1986, 1989).

Nevertheless, there are still many aspects of the hydraulics of layered flows that require further investigation. This paper will address three interrelated issues: (i) the relaxation of the Boussinesq approximation, that the relative density difference between the layers is small; (ii) the derivation and use of *appropriate* Froude numbers to characterize layered flows; and (iii) flows where the hydraulic equations yield imaginary phase speeds for long internal waves. The primary focus will be on

steady two-layer flows; but, the results can, in principle, be extended to any number of layers.

The characteristic velocities (celerities) of long waves, of infinitesimal amplitude, both on the free surface, and on the interface, can be determined from the one-dimensional equations. The celerity of a long wave is the sum of a convective velocity and a phase speed. The Froude number is generally defined as the ratio of the convective velocity to the phase speed. An alternative, see Armi (1986), is to define the Froude number in terms of conditions at special locations, traditionally called 'hydraulic controls'. For single-layer flow there is no difficulty, since both definitions yield the same Froude number. However, different Froude numbers result when these definitions are applied to two-layer flow. The present paper seeks to remove the possibility of confusion by discussing the significance of these Froude numbers, and deriving the fundamental equation interrelating them. Both unidirectional and exchange flow through a contraction are analysed to illustrate this interrelationship.

The celerity of long internal waves in a two-layer flow was determined by Stokes (1847, see Gill 1982, p. 121) for the special case of equal velocity in each layer. The solution for both external and internal waves in a flow satisfying the Boussinesq approximation was given by Schijf & Schönfeld (1953). This solution is often accurate even when the relative density difference is not small. However, it will be shown that there are also situations where the non-Boussinesq solution is required no matter how small the relative density difference. A quartic equation must be solved to obtain the non-Boussinesq long-wave celerities. Even though the general solution for quartic equations is algebraically complex, and is therefore rarely used in favour of a numerical solution, it will be used in the present paper, since it facilitates a more complete understanding the hydraulics of two-layer flows.

Armi & Farmer's (1986) analysis of Boussinesq exchange flow through a contraction is extended to show that in a significant portion of the flow the celerities are imaginary, corresponding to the instability of long waves (Long 1956). On the basis of conditions at the narrowest section Armi & Farmer (1986) incorrectly concluded that instability does not occur. They did not check the stability on either side of the narrowest section. It is shown in the present paper, that in both Boussinesq and non-Boussinesq exchange flow through a contraction imaginary solutions may occur to one side of the narrowest section, but not at the narrowest section.

The hydraulics of layered flows is reviewed in §2. The fundamental equation interrelating the Froude numbers relevant to two-layer flows is derived in §3, and illustrated using unidirectional two-layer flow through a contraction as an example. Boussinesq and non-Boussinesq exchange flows through a contraction are analysed in §4. The results are summarized in §5.

2. Review of the hydraulics of layered flows

Three assumptions, known as the hydraulic assumptions, are used in the study of layered flows. They are: (i) the fluids are inviscid; (ii) the pressure is hydrostatic; and (iii) within each layer the density is constant and the velocity varies only in the flow direction. Armi (1975, 1986) presents the hydraulic equations in the general form:

$$\frac{\partial \boldsymbol{v}}{\partial t} + \boldsymbol{C}\frac{\partial \boldsymbol{v}}{\partial x} = \boldsymbol{D}\frac{\partial \boldsymbol{f}}{\partial x}, \tag{1}$$

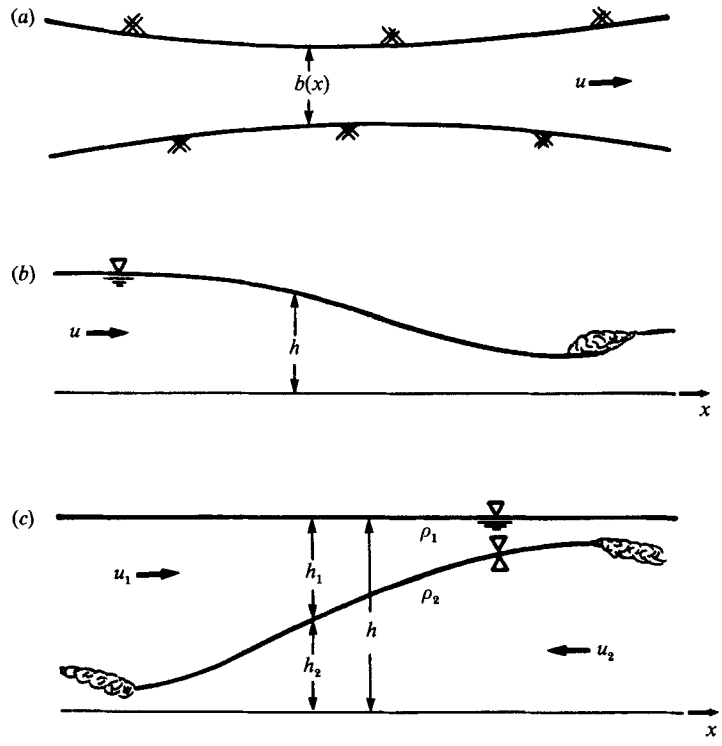

FIGURE 1. (*a*) Plan view for flow through a contraction, and side views for (*b*) single-layer flow, and (*c*) a two-layer exchange flow.

where x is the horizontal coordinate and t is time. In general the variables on the left-hand side of (1) are unknown, and the variables on the right-hand side are known. If the flow has j layers: $\boldsymbol{v}$ is a vector with $2j$ elements; $\boldsymbol{f}$ is a vector with 2 elements; $\boldsymbol{C}$ is a $2j \times 2j$ matrix; and $\boldsymbol{D}$ is an $2 \times 2j$ matrix. Armi (1986) shows that for single-layer flow

$$\boldsymbol{C} = \begin{bmatrix} u & g \\ h & u \end{bmatrix}, \quad \boldsymbol{v} = \begin{bmatrix} u \\ h \end{bmatrix}, \quad \boldsymbol{D} = \begin{bmatrix} -g & 0 \\ 0 & Q \end{bmatrix}, \quad \boldsymbol{f} = \begin{bmatrix} h_s \\ b^{-1} \end{bmatrix}, \tag{2}$$

and for two-layer flow with a free surface:

$$\boldsymbol{C} = \begin{bmatrix} u_1 & 0 & g & g \\ 0 & u_2 & (1-\epsilon)g & g \\ h_1 & 0 & u_1 & 0 \\ 0 & h_2 & 0 & u_2 \end{bmatrix}, \quad \boldsymbol{v} = \begin{bmatrix} u_1 \\ u_2 \\ h_1 \\ h_2 \end{bmatrix}, \quad \boldsymbol{D} = \begin{bmatrix} -g & 0 \\ -g & 0 \\ 0 & Q_1 \\ 0 & Q_2 \end{bmatrix}, \quad \boldsymbol{f} = \begin{bmatrix} h_s \\ b^{-1} \end{bmatrix}, \tag{3}$$

where u_n, h_n, ρ_n, and Q_n are the velocity, thickness, density, and volumetric flow rate of layer n, as indicated on figure 1, and g is the gravitational acceleration. Subscript 1 refers to the upper layer, and subscript 2 refers to the lower layer; for single-layer flow no subscripts are used. The variations in bottom elevation and channel width are $h_s(x)$ and $b(x)$ respectively. For the examples considered in the present paper only variations in width will be considered, so that $h_s(x) = 0$. The relative density difference $\epsilon \equiv (\rho_2 - \rho_1)/\rho_2$. If $\epsilon \ll 1$, the flow is said to be Boussinesq. For the pressure to be hydrostatic the variations in channel width and depth must be gradual.

2.1. *Characteristic velocities, Froude numbers, critical flow, and hydraulic controls*

As a consequence of the assumption of hydrostatic pressure, the hydraulic equations (1) have only long-wave solutions. The characteristic velocities (celerities), λ, of these long waves are specified by the eigenvalue equation:

$$\mathrm{Det}\,(\boldsymbol{C}-\lambda \boldsymbol{I}) = 0, \tag{4}$$

where $\boldsymbol{I}$ is the identity matrix. The characteristic velocities are given by:

$$\lambda^{\pm} = u_{\mathrm{con}} \pm c. \tag{5}$$

The ratio of the convective velocity, u_{con}, to the phase speed, c, is traditionally known as the Froude number. When the matrix $\boldsymbol{C}$ for single-layer flow (2) is substituted into the eigenvalue equation (4), (5) yields, $u_{\mathrm{con}} = u, c = (gh)^{\frac{1}{2}}$, and the Froude number

$$F = \frac{u}{(gh)^{\frac{1}{2}}}. \tag{6}$$

This Froude number is analogous to the Mach number in gas flow. The flow is said to be supercritical, critical, or subcritical depending on whether F^2 is greater than, equal to, or less than unity. It is customary to use F^2 rather than F, since it is F^2 that appears in the solutions of the hydraulic equations, see (7) below. If a device, such as a sluice gate or a weir, is used to control the flow in a channel, there is an abrupt change from subcritical flow upstream, to supercritical flow downstream, of the control device. So it is customary to call any location where a flow changes from subcritical to supercritical a *hydraulic control*, or simply, a *control*. This paper considers channels of gradually varying width in which the flow passes smoothly from subcritical to supercritical flow. In such channels the flow is always critical at the point of control.

The above principles have been applied to multi-layered flows by Benton (1954), and Baines (1988). The essential difference being that long waves can propagate along each interface as well as the free surface. Therefore, j Froude numbers based on the characteristic velocities can be defined for a j layered flow. However, even for two-layer flows these Froude numbers are not readily determined except in special cases. It is perhaps for this reason that Froude numbers based on characteristic velocities have not previously been used in studies of multi-layered flows. Instead Froude numbers have been defined in a variety of ways, many of which have been specific to particular experiments; however, a second general method of defining Froude numbers arises from the steady solutions of the hydraulic equations.

2.2. *Steady solutions and the composite Froude number*

Consider the solution of the hydraulic equation (1) for the depth of steady single-layer flow through a contraction:

$$\frac{1}{h}\frac{\mathrm{d}h}{\mathrm{d}x} = \frac{F^2}{1-F^2}\frac{1}{b}\frac{\mathrm{d}b}{\mathrm{d}x}. \tag{7}$$

At points of hydraulic control $F^2 = 1$, so to avoid infinite convective accelerations, $\mathrm{d}b/\mathrm{d}x = 0$. The requirement, $\mathrm{d}b/\mathrm{d}x = 0$, determines the possible locations of hydraulic control. The requirement, $F^2 = 1$, determines the depth of flow at a control, $h_{\mathrm{c}} = (Q/gb^2)^{\frac{1}{3}}$. In any flow there may be more than one possible control location. A classification scheme is often needed to identify, for any given set of

conditions, those locations that are acting as controls. Lawrence (1985, 1987) presents classification schemes for steady single- and two-layer flow over an obstacle.

The steady solutions to the hydraulic equations (1) can be written in the general form:

$$\frac{\mathrm{d}\boldsymbol{v}}{\mathrm{d}x} = \frac{\boldsymbol{R}}{\mathrm{Det}\,\boldsymbol{C}}, \tag{8}$$

where $\boldsymbol{R} = (\mathrm{Adj}\,\boldsymbol{C})\boldsymbol{D}(\mathrm{d}f/\mathrm{d}x)$. Solutions exist if the matrix $\boldsymbol{C}$ is non-singular ($\mathrm{Det}\,\boldsymbol{C} \neq 0$), or, if at locations where the singularity condition, $\mathrm{Det}\,\boldsymbol{C} = 0$, is satisfied, the regularity condition, $\boldsymbol{R} = 0$, is also satisfied. If $\mathrm{Det}\,\boldsymbol{C} = 0$, then from the eigenvalue equation (4) $\lambda = 0$, so that locations where the singularity condition is satisfied must also be controls. At controls the values of the dependent variables, represented by $\boldsymbol{v}$, can be determined using the regularity conditions ($\mathrm{d}b/\mathrm{d}x = 0$, in the above example), and singularity conditions ($F^2 = 1$, in the above example). Once $\boldsymbol{v}$ is known at a control the steady solutions (8) can be used directly, but is generally integrated to give an energy (Bernoulli) equation for each layer. For two-layer flow:

$$H_1 = h_1 + h_2 + h_s + \frac{u_1^2}{2g}, \tag{9a}$$

$$H_2 = (1-\epsilon)h_1 + h_2 + h_s + \frac{u_2^2}{2g}, \tag{9b}$$

where the reduced gravitational acceleration, $g' = \epsilon g$. To emphasize the internal dynamics it is most convenient† to define an energy difference, $\Delta H \equiv (H_1 - H_2)/\epsilon$, i.e.:

$$\Delta H = h_1 + (u_1^2 - u_2^2)/2g'. \tag{10}$$

Equations (9) and (10) are used to obtain the solutions presented in §3 and §4.

Applying the general solution (8) to steady, two-layer flow through a contraction yields:

$$\begin{bmatrix} \dfrac{\mathrm{d}h_1}{\mathrm{d}x} \\ \dfrac{\mathrm{d}h_2}{\mathrm{d}x} \end{bmatrix} = \frac{1}{1-G^2} \begin{bmatrix} h_1\left\{G^2 - \left(1+\dfrac{h_2}{h_1}\right)F_2^2\right\} \\ h_2\left\{G^2 - \left(1+(1-\epsilon)\dfrac{h_1}{h_2}\right)F_1^2\right\} \end{bmatrix} \frac{1}{b}\frac{\mathrm{d}b}{\mathrm{d}x}. \tag{11}$$

In this case the singularity condition is $G^2 = 1$, where Armi (1986) defines the composite Froude number:

$$G^2 \equiv F_1^2 + F_2^2 - \epsilon F_1^2 F_2^2, \tag{12a}$$

where

$$F_n^2 \equiv u_n^2/g'h_n, \tag{12b}$$

are the densimetric Froude numbers of the individual layers. From (11) we see that if $G^2 = 1$, hydraulic control may be achieved in two ways: either $\mathrm{d}b/\mathrm{d}x = 0$, (in this case the term *topographic control* will be used); or

$$\left(1+\frac{h_2}{h_1}\right)F_2^2 = \left(1+(1-\epsilon)\frac{h_1}{h_2}\right)F_1^2, \tag{13}$$

in this case the term *virtual control* is used, following Wood (1968).

† Various authors (see Lawrence 1985; Armi 1986; Denton 1987) have used

$$\Delta H = h_2 + h_s + \{u_2^2 - (1-\epsilon)u_1^2\}/2g',$$

which is an alternative to (10), but more cumbersome to use in the study of non-Boussinesq flows.

The composite Froude number G^2 may determine the criticality of two-layer flow just as the parameter F^2 determines the criticality of single-layer flow. However, a two-layer flow supports both internal and external waves with different characteristic velocities. It is not immediately obvious how the single parameter, G^2, can determine the criticality of two-layer flows, since it cannot be the ratio of convective velocity to phase speed for both internal and external waves. This dilemma is resolved in the following section by deriving the equation relating the Froude numbers based on the characteristic velocities to the composite Froude number.

3. Two-layer Froude numbers and the relationship between them

The characteristic velocities from which Froude numbers are derived are the solutions to the eigenvalue equation (4). In a two-layer system they can be written as:

$$\lambda_{\mathrm{E}}^{\pm} = u_{\mathrm{E}} \pm c_{\mathrm{E}}, \tag{14a}$$

$$\lambda_{\mathrm{I}}^{\pm} = u_{\mathrm{I}} \pm c_{\mathrm{I}}. \tag{14b}$$

The external characteristic velocities, $\lambda_{\mathrm{E}}^{\pm}$, correspond to external (free surface) wave motions; and the internal characteristic velocities, $\lambda_{\mathrm{I}}^{\pm}$, correspond to internal (interfacial) wave motions. The convective velocities, u_{E} and u_{I}, and the phase velocities, c_{E} and c_{I}, are given by:

$$u_{\mathrm{E}} = \bar{u} + \zeta(z_1)^{\frac{1}{2}}, \quad c_{\mathrm{E}} = (z_3)^{\frac{1}{2}} + (z_2)^{\frac{1}{2}}, \tag{15a}$$

$$u_{\mathrm{I}} = \bar{u} - \zeta(z_1)^{\frac{1}{2}}, \quad c_{\mathrm{I}} = (z_3)^{\frac{1}{2}} - (z_2)^{\frac{1}{2}}, \tag{15b}$$

where $\zeta = \mathrm{sgn}\,(u_2 - u_1)$, and the arithmetic mean velocity $\bar{u} = \frac{1}{2}(u_1 + u_2)$. z_1, z_2 and z_3 are the roots of a cubic derived from the quartic equation specified by the eigenvalue equation (4). The details are given in the Appendix.

Whether the internal phase speed given in (15b) is real or not depends on the value of the stability Froude number:

$$F_{\Delta}^2 \equiv \frac{(u_2 - u_1)^2}{g'h}, \tag{16}$$

where $h = h_1 + h_2$, is the total depth of flow. Imaginary internal phase speeds result when the stability Froude number exceeds a critical value, $(F_{\Delta}^2)_{\mathrm{crit}}$. The variation of $(F_{\Delta}^2)_{\mathrm{crit}}$ as a function of both ϵ and $\alpha \equiv 4h_1 h_2/h^2$ is plotted in figure 2. In all cases $1 < (F_{\Delta}^2)_{\mathrm{crit}} < 2$; and for Boussinesq flows $(F_{\Delta}^2)_{\mathrm{crit}} \approx 1$ (for the remainder of this paper the symbol $\approx$ will be used to indicate that the Boussinesq approximation has been made). The requirement that $F_{\Delta}^2 \leqslant (F_{\Delta}^2)_{\mathrm{crit}}$ for the stability of long waves will be referred to as Long's stability criterion, after Long (1956).

Dividing convective velocities by phase speeds given in (15) yields:

$$F_{\mathrm{E}} = \frac{\bar{u} + \zeta(z_1)^{\frac{1}{2}}}{(z_3)^{\frac{1}{2}} + (z_2)^{\frac{1}{2}}}, \tag{17a}$$

$$F_{\mathrm{I}} = \frac{\bar{u} - \zeta(z_1)^{\frac{1}{2}}}{(z_3)^{\frac{1}{2}} - (z_2)^{\frac{1}{2}}}. \tag{17b}$$

A glance at Appendix 1 reveals that it is not a simple matter to evaluate these Froude numbers exactly. However, in many cases the Boussinesq approximations presented below are sufficiently accurate, an exception is discussed in §4.

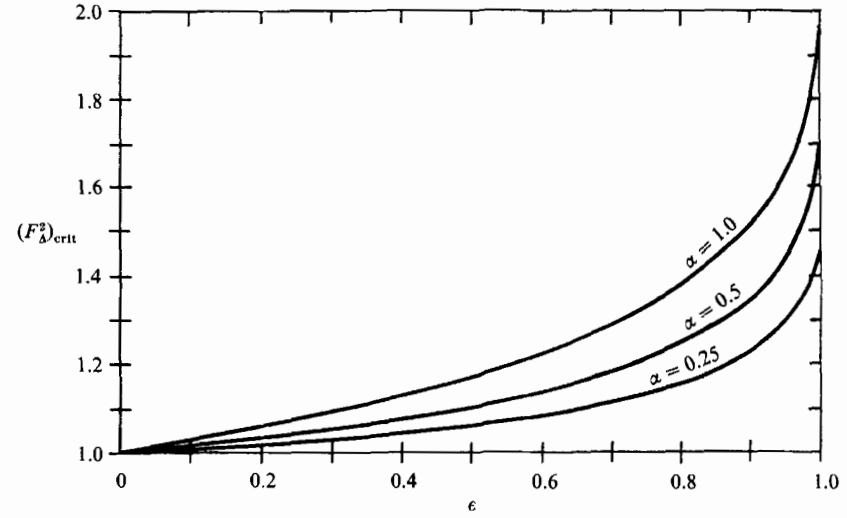

FIGURE 2. The maximum value of the stability Froude number, $(F_\Delta^2)_{\text{crit}}$, as a function of the relative density difference, ϵ, for $\alpha = 0.25$, 0.5, and 1.0, where $\alpha = 4h_1 h_2/h^2$.

3.1. *Boussinesq approximations*

Expanding the expressions for z_1, z_2 and z_3 derived in the Appendix in powers of ϵ gives:

$$z_1 = \tfrac{1}{4}gh\{\epsilon(1-\alpha)F_\Delta^2 + O(\epsilon^2)\}, \tag{18a}$$

$$z_2 = \tfrac{1}{4}gh\{1-(\epsilon\alpha(1-F_\Delta^2))^{\frac{1}{2}} + \tfrac{1}{2}\epsilon\alpha F_\Delta^2 + O(\epsilon^{\frac{3}{2}})\}, \tag{18b}$$

$$z_3 = \tfrac{1}{4}gh\{(1+(\epsilon\alpha(1-F_\Delta^2))^{\frac{1}{2}} + \tfrac{1}{2}\epsilon\alpha F_\Delta^2 + O(\epsilon^{\frac{3}{2}})\}. \tag{18c}$$

Substituting into the expressions for the convective velocities and phase speeds (15) yields the Boussinesq results of Schijf & Schönfeld (1953), i.e.:

$$u_{\text{E}} \approx \frac{u_1 h_1 + u_2 h_2}{h}, \quad c_{\text{E}} \approx (gh)^{\frac{1}{2}}, \tag{19a}$$

$$u_{\text{I}} \approx \frac{u_1 h_2 + u_2 h_1}{h}, \quad c_{\text{I}} \approx \left(\frac{g' h_1 h_2}{h}(1-F_\Delta^2)\right)^{\frac{1}{2}}. \tag{19b}$$

Dividing the internal convective velocity by the internal phase speed, Lawrence (1985) obtained the internal Froude number:

$$F_{\text{I}} \approx \frac{u_1 h_2 + u_2 h_1}{(g' h h_1 h_2 (1-F_\Delta^2))^{\frac{1}{2}}}, \tag{20a}$$

and after some rearrangement,

$$F_{\text{I}}^2 \approx \frac{G^2 - F_\Delta^2}{1-F_\Delta^2}. \tag{20b}$$

The external Froude number is:

$$F_{\text{E}} \approx \frac{\tilde{u}}{(gh)^{\frac{1}{2}}}, \tag{21}$$

where the flow weighted mean velocity $\tilde{u} = (u_1 h_1 + u_2 h_2)/h$. The external Froude number for Boussinesq two-layer flows is the same as the Froude number for single-layer flows. This is as we would expect (see Armi 1986), since if the density difference between the layers is small, a long free surface wave should behave as if the fluid were of uniform density. It is demonstrated in §4.2 that the Froude number for non-Boussinesq two-layer flows is not equal to the single-layer Froude number, see figure 11.

A further simplification to the Boussinesq solution is to consider: either, flows with $u_1 \gg u_2$, and $h_1 \ll h_2$, so that $F_1^2 \gg F_2^2$; or, flows with $u_1 \ll u_2$, and $h_1 \gg h_2$, so that $F_1^2 \ll F_2^2$. In both cases $F_\Delta^2 \ll 1$, and the expression for the internal Froude number (20*b*) simplifies to

$$F_1^2 \approx F_n^2, \tag{22}$$

which is the anticipated, and the frequently used, result (see Turner 1973, §3.2). The layer with the much higher Froude number is called the active layer; the other layer is called the passive layer, and its dynamics can be ignored, see Armi (1986). This case emphasizes the need to distinguish between the two convective velocities u_E and u_I. If u_1 were equal to u_E we would obtain an internal Froude number which would depend, unrealistically, on conditions in the passive layer.

3.2. *Unidirectional two-layer flow through a contraction*

The results of the analysis of steady, unidirectional, two-layer flow through a contraction will be used to illustrate the above results. The exact nature of the flow is dependent on: the relative density difference, ϵ; the flow rate ratio, $q_r = q_1/q_2$; and the width of the contraction, $b(x)$. The solution for the case where $\epsilon = 0.5$, $q_r = 1$, and $b^*(x) = b(x)/b(0) = 1+x$, is presented in figure 3. A plan view of the contraction is given in figure 3(*a*). The exact solutions for the interface and free surface elevations are plotted in figure 3(*b*), and the exact solutions for $G^2(x)$, $F_I^2(x)$, $F_E^2(x)$ and $F_\Delta^2(x)$ are plotted in figure 3(*c*). Although a large value of ϵ was chosen for the sake of clarity in the plots, the variations are qualitatively the same for all values of ϵ and q_r. They are:

(i) F_E^2, increases monotonically from zero far upstream to unity at the exit;

(ii) F_I^2, increases monotonically from zero far upstream, to unity at the internal control, located where

$$b \approx \left(\frac{64}{27\epsilon}\frac{1+q_r^2)}{(1+q_r)^2}\right)^{\frac{1}{3}},$$

to a value of $\approx 4/\epsilon$ at the exit;

(iii) F_Δ^2, also increases monotonically in the flow direction, to a maximum $\approx \frac{1}{4}\epsilon[q_r/1+q_r]^2$.

(iv) G^2 increases from zero far upstream, to a value of unity at the internal control, to a maximum value of $\approx 1/\epsilon$ just upstream of the exit, and then plunges to a value of unity at the external control. This variation can only be fully understood once the relationship between the various Froude numbers is known, see §3.3.

Some of the above results are also conveniently represented in figure 3(*d*) using the Froude number plane used by Benton (1954) and Armi (1986). The flow proceeds from the origin of the Froude number plane, along a straight line of slope $1/u_r^3$ that cuts the curve $F_I^2 = G^2 = 1$ (at a point corresponding to the virtual control), and intersects the line $F_E^2 = G^2 = 1$ (at a point corresponding to the exit control). The variation of the velocity ratio u_r with ϵ for various values of q_r is plotted in figure 4.

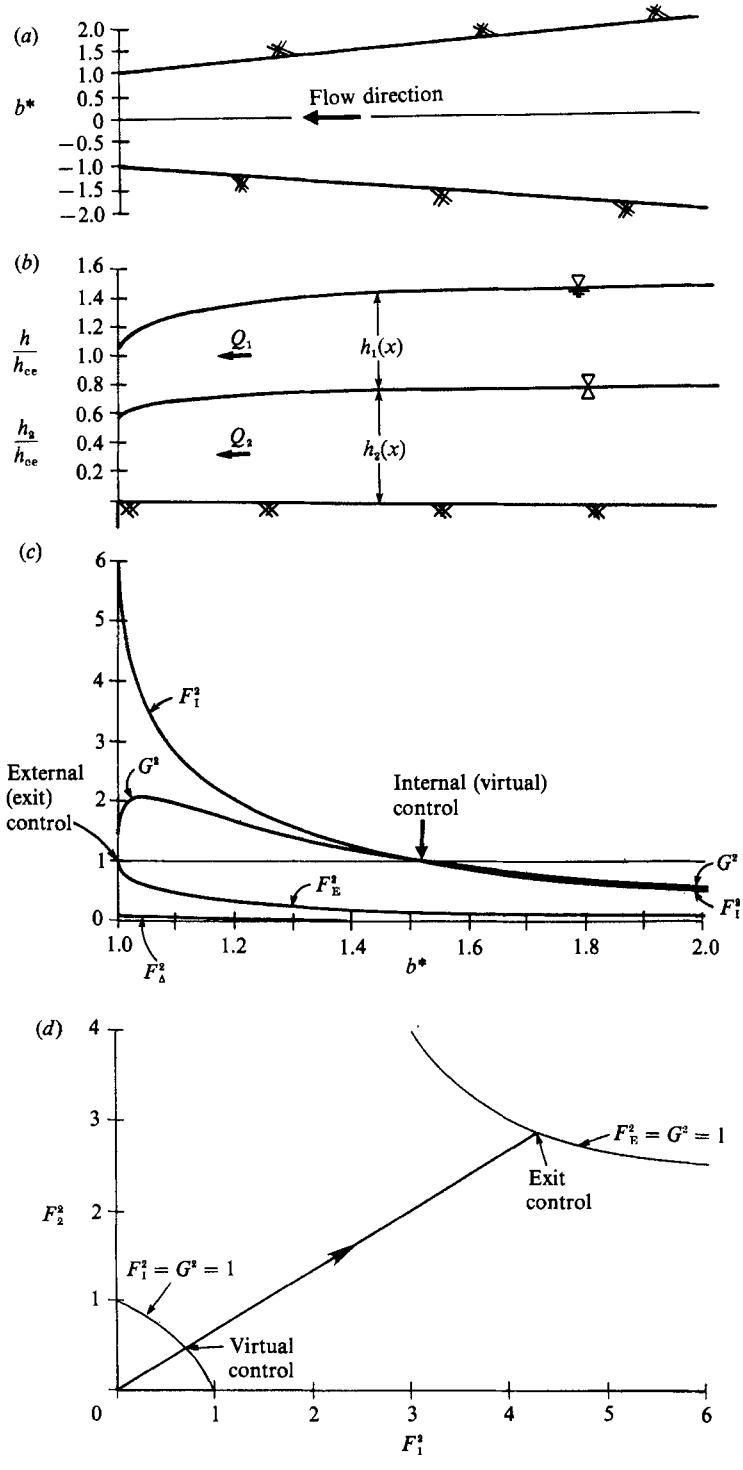

FIGURE 3. Exact solution for unidirectional flow through a contraction with the flow rate ratio, $q_r = 1$, the relative density difference, $\epsilon = 0.5$, and the width ratio, $b^* = b(x)/b(0) = 1+x$. (*a*) Plan view of the contraction. (*b*) Variation of the free surface and interface elevations expressed relative to, the critical depth at the exit, $h_{ce} = [(Q_1+Q_2)^2/gb(0)^2]^{\frac{1}{3}}$. (*c*) Variation of F_E^2, F_I^2, F_Δ^2 and G^2. (*d*) Representation of the flow on the Froude number plane.

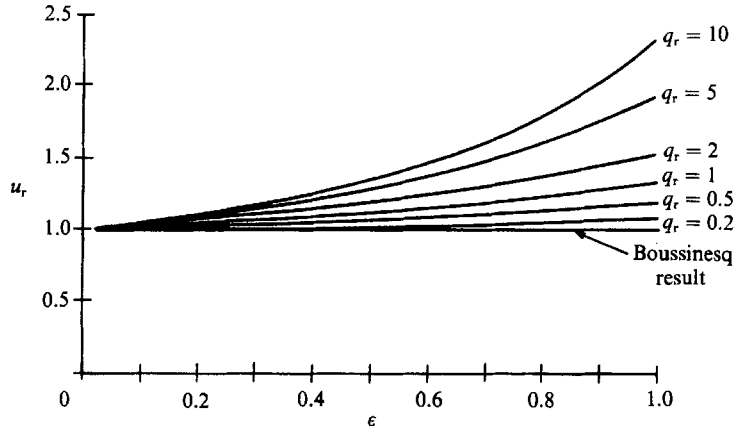

FIGURE 4. Variation of the velocity ratio $u_r = u_1/u_2$, as a function of the relative density difference, ϵ, for various values of the flow rate ratio, $q_r = Q_1/Q_2$.

It follows from the solutions for steady unidirectional two-layer flow through a contraction ((11) and (13)) that for fixed q_r and ϵ, the velocity ratio u_r is constant.

3.3. *Fundamental relationship between Froude numbers*

Since the determinant of a matrix is the product of its eigenvalues, we can write $\mathrm{Det}\,\boldsymbol{C} = \lambda_E^+ \lambda_I^+ \lambda_I^- \lambda_E^-$. In addition, taking the determinant of the matrix $\boldsymbol{C}$ for two-layer flows (3), and applying the definition of G^2 (equation (12a)), gives $\mathrm{Det}\,\boldsymbol{C} = \epsilon g^2 h_1 h_2 (1-G^2)$. Equating these two expressions for $\mathrm{Det}\,\boldsymbol{C}$, and using the equation for the characteristic velocities (5), gives:

$$(1-G^2) \approx k(1-F_E^2)(1-F_I^2), \tag{23}$$

where $k = c_I^2 c_E^2/\epsilon g^2 h_1 h_2 \approx 1-F_\Delta^2$. Equation (23) is the fundamental relationship between the Froude numbers relevant to two-layer flows. If $k > 0$, (23) tells us that at a control location (i.e. where $G^2 = 1$), the flow may be internally critical, $F_I^2 = 1$, or externally critical, $F_E^2 = 1$, and Armi's (1986) introduction of the term composite Froude number is most appropriate. However, in the absence of any other information, the value of the composite Froude number only gives us a limited appreciation of the nature of the flow. All we can say is that:

(i) if $G^2 > 1$, then the flow may be stable, internally supercritical, and externally subcritical; or it may be unstable, since if

$$c_I^2 < 0, \quad \text{then} \quad k < 0, F_I^2 < 0, \quad \text{and} \quad G^2 > 1.$$

Some unstable flows are considered in §4;

(ii) if $G^2 = 1$, then the flow is either internally critical, externally critical, or marginally stable;

(iii) if $G^2 < 1$, then the flow is either both externally subcritical and internally subcritical, or both externally supercritical and internally supercritical. Note that in the later case G^2 may even take on negative values.

Often more information is available than just the value of G^2, and any ambiguities as to the criticality of the flow can be resolved. For instance in unidirectional flow through a contraction $k \approx 1$, so we can write:

$$(1-G^2) \approx (1-F_E^2)(1-F_I^2). \tag{24}$$

This relationship is shown in figure 3(*c*). Knowledge of the value of G^2 is sufficient to determine the criticality of the flow since $F_E^2 \leqslant 1$ throughout the contraction. When the flow is internally supercritical, $1 < G^2 < F_I^2$, and when the flow is internally subcritical, $F_I^2 < G^2 < 1$, as can be seen in figure 3(*c*). In many other flows of interest, e.g. exchange flow through a contraction and two-layer flow over an obstacle, $F_E^2 \approx 0$, and

$$(1-G^2) \approx (1-F_\Delta^2)(1-F_I^2), \tag{25}$$

giving

$$F_I^2 \approx \frac{G^2-F_\Delta^2}{1-F_\Delta^2}, \tag{20b}$$

and again G^2 correctly specifies the criticality of the flow.

Although G^2 often determines the criticality of the flow, there are situations where this knowledge is insufficient. For example, we cannot use G^2 to describe the behaviour of the oblique standing waves that can form in supercritical layered flow, as seen in space shuttle photographs of Gibraltar Strait, see Farmer & Armi (1986, figure 20). These oblique waves are analogous to those found in single-layer flows (Henderson 1966, pp. 239–250), and to Mach waves found in gas flow (Prandtl 1952, pp. 275–277). A situation where the determination of the Mach angle is of importance is illustrated in the experiments of Lawrence (1985). In these experiments, two-layer flows over an obstacle with internally supercritical flow downstream of the crest were produced. Shear instabilities that form on the interface generate in considerable mixing between the layers. These instabilities are strongest in a region bounded by the sidewalls and oblique (Mach) waves that form at an angle to the sidewalls. The angle that they make with the sidewalls is given by $\arcsin(1/F_I)$. Thus, F_I is needed for the prediction of mixing, and the value of G^2 is of little relevance.

4. Exchange flow through a contraction

Unidirectional flow through a contraction was chosen for analysis in §3, since it illustrates the relationship between the internal, external, and composite Froude numbers, as well as some of the consequences of relaxing the Boussinesq approximation. However, the significance of the stability Froude number was not discussed, since it is only of $O(\epsilon)$ in unidirectional flow through a contraction. The significance of F_Δ^2, and the possibility, and consequences, of attaining values in violation of Long's stability criterion, in both Boussinesq and non-Boussinesq flows, will now be investigated. The following non-dimensional quantities are used:

$$y_n \equiv \frac{h_n}{H_1}, \quad u_n^* \equiv \frac{u_n}{(g'H_1)^{\frac{1}{2}}}, \quad q_n \equiv \frac{Q_n}{(g'b_0^2H_1^3)^{\frac{1}{2}}}, \quad (n=1,2), \tag{26}$$

where H_1 is the Bernoulli constant for the upper layer, see (9a), and b_0 is the minimum width of the contraction. The subscript 0 is used to indicate conditions at the narrowest section (throat) of the contraction. Substituting the definitions given in (26) into the definition of the stability Froude number (16) gives:

$$F_\Delta^2 = (q_2/b^*y_1y_2)^2(q_ry_2+y_1)^2, \tag{27}$$

where the relative width of the channel $b^* = b/b_0$. By convention, flows from left-to-right are positive, so for the example given in figure 1(*c*), Q_2 and u_2 are negative. The flow rate ratio $q_r = |Q_1|/|Q_2|$.

Two further equations are needed to specify the variation in free surface and

interface heights. The first is the dimensionless Bernoulli equation for the upper layer:

$$y_1 + y_2 + \tfrac{1}{2}\epsilon u_1^{*2} = 1. \tag{28}$$

The second is the dimensionless energy difference between the layers:

$$\Delta H^* \equiv \Delta H/H_1 = y_1 + \tfrac{1}{2}(u_1^{*2} - u_2^{*2}). \tag{29}$$

From this point on the * superscripts will be dropped.

Boussinesq exchange flow through a contraction has already been studied in some detail by Armi & Farmer (1986, hereinafter referred to as AF). Only maximal exchange flows; i.e. flows with both a topographic control (located at the throat), and a virtual control (located in the vicinity of, but not necessarily at, the throat), will be considered. AF showed that for all values of q_r Long's stability criterion is satisfied at the throat of the contraction, but they did not present results for any other sections. AF's analysis will first be extended to provide a complete description of Boussinesq flows at all sections of the contraction. Although AF resorted to numerical solutions, this is not essential in Boussinesq flows, and algebraic expressions for all the parameters of interest are derived below. The analysis will then be extended to obtain solutions for the case of non-Boussinesq flows.

4.1. *Boussinesq exchange flow through a contraction*

The variation of F_Δ^2 is best illustrated using the Froude number plane. This involves expressing F_Δ^2 in terms of F_1^2 and F_2^2. For Boussinesq flows with a negligible free-surface deflection

$$y_1 + y_2 \approx 1, \tag{30}$$

which together with the definition of the densimetric Froude numbers (12*b*), yields:

$$F_\Delta^2 \approx \frac{F_1^{\frac{2}{3}} F_2^{\frac{2}{3}} (q_r^{\frac{1}{3}} F_1^{\frac{2}{3}} \pm F_2^{\frac{2}{3}})^2}{F_1^{\frac{2}{3}} + q_r^{\frac{2}{3}} F_2^{\frac{2}{3}}}. \tag{31}$$

Contours of F_Δ^2 are plotted on the Froude number plane for $q_r = 1$ in figure 5. Two aspects of these plots need to be emphasized:

(i) There are significant portions of the Froude number plane where Long's stability criterion is violated.

(ii) For $q_r = 1$, the fact that Long's stability criterion is only violated when $G^2 > 1$, is shown in figure 5. This result is seen to apply for all values of q_r by expanding F_Δ^2 and G^2 in terms of q_r, y_1 and y_2 to obtain:

$$\frac{F_\Delta^2}{G^2} \approx 1 - \frac{(q_r y_2^2 - y_1^2)^2}{q_r^2 y_2^3 + y_1^3}. \tag{32}$$

So $F_\Delta^2 \leqslant G^2$ no matter what the values of q_r, y_1 and y_2. This result indicates that all internally subcritical flows satisfy Long's stability criterion.

The possibility of exchange flow violating Long's stability criterion will now be investigated. AF show that if q_r is respectively less than, equal to, or greater than unity, then there is a virtual control downstream of, at, or upstream of, the throat. At the virtual control:

$$u_{1v} \approx -u_{2v}, \tag{33}$$

and

$$\Delta H_v \approx q_r/(1+q_r). \tag{34}$$

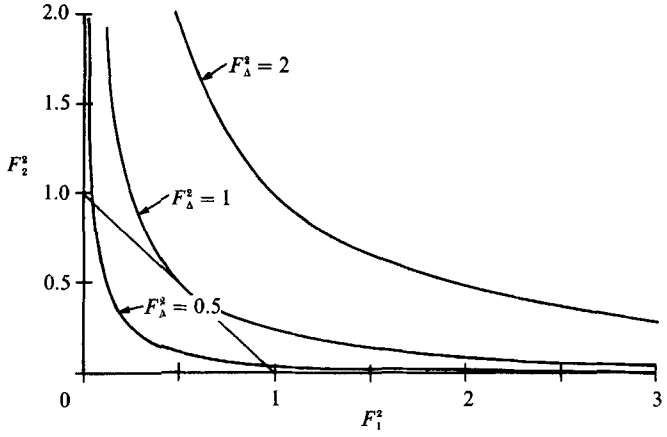

FIGURE 5. Contours of F_Δ^2 in the Froude number plane for Boussinesq exchange flows with $q_r = 1$.

The subscript v is used to indicate conditions at the virtual control. AF assume that ΔH is conserved in the region of flow between any internal hydraulic jumps that may occur, as indicated in figure 1(*c*). In this region, which must include both the virtual and topographic controls, $\Delta H = \Delta H_v$. Substituting (33) and (34) into the definition of ΔH (29), yields:

$$\left\{\frac{q_2}{b}\right\}^2 \approx \frac{2(y_1 y_2)^2}{(1+q_r)(y_1+q_r y_2)}. \tag{35}$$

Assuming no free-surface deflection, and substituting (35) into the expression for F_Δ^2 (27) gives:

$$F_\Delta^2 \approx \frac{2\{1-(1-q_r)y_2\}}{1+q_r}. \tag{36}$$

The variation of F_Δ^2 with y_2 for various values of q_r is plotted in figure 6. Note that, if $q_r = 1$ the flow is marginally stable ($F_\Delta^2 = 1$) throughout. If $q_r \neq 1$ a moderately barotropic flow attains marginal stability when $y_2 \approx 0.5$, and becomes unstable when the layer with the higher flow rate becomes the thinner of the two layers. The overall limiting value of $F_\Delta^2 \approx 2$, as can be inferred from figure 6.

For a more complete understanding of exchange flow through a contraction it is important to determine the thickness of the layers, and the width of the channel, at three locations:

(i) at the virtual control (y_{2v} and b_v);
(ii) at the position where the flow is marginally stable (y_{2m} and b_m);
(iii) at the throat (y_{20} and b_0).

Only two of the above heights and widths are constants: $b_0 = 1$ by definition; and $y_{2m} = 0.5$, see the expression for F_Δ^2 (equation (36)) and figure 6. The condition that the layer velocities are equal in magnitude (equation (33)), gives $y_{2v} \approx 1/(1+q_r)$. The remaining variables, y_{20} and b_v, have previously been evaluated numerically, see figure 5 in AF. The derivation of algebraic expressions for y_{20}, b_m, and b_v is presented below for the first time.

The height of the interface at the throat is determined by using the fact that b has a minimum value at the throat, in conjunction with the expression for q_2/b (equation (35)), to obtain:

$$3(q_r-1)y_{20}^2+(5-q_r)y_{20}-2 \approx 0. \tag{37}$$

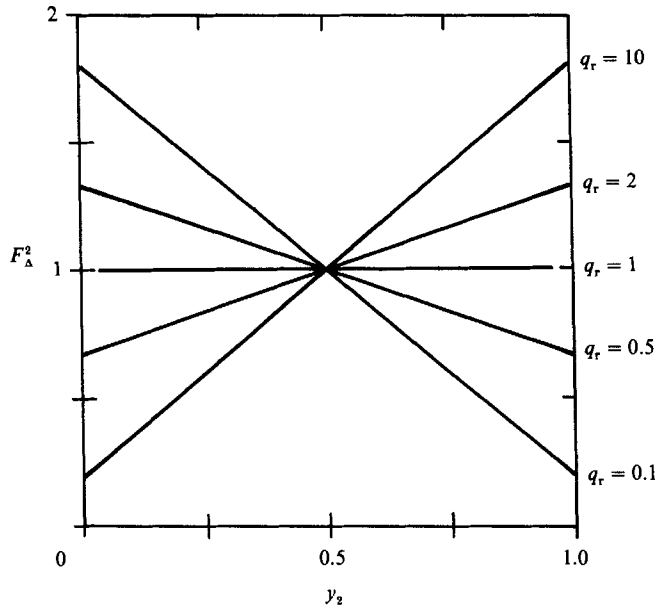

FIGURE 6. Variation of F_Δ^2 with the dimensionless interface height y_2 for exchange flow through a constriction.

Solving (37) for $q_r = 1$ gives $y_{20} \approx 0.5$. Recall that in addition if $q_r = 1$, then $y_{2v} \approx y_{2m} \approx 0.5$, so that the flow is both critical and marginally stable at the throat, as noted by AF. Solving (37) for $q_r \neq 1$ gives:

$$y_{20} \approx \frac{q_r - 5 + (q_r^2 + 14q_r + 1)^{\frac{1}{2}}}{6(q_r - 1)}, \tag{38}$$

and

$$q_2 \approx \left(\frac{2\gamma}{1+q_r}\right)^{\frac{1}{2}}, \tag{39}$$

where

$$\gamma = \frac{((1-y_{20})\,y_{20})^2}{1-(1-q_r)\,y_{20}}.$$

An expression for the width of the constriction, obtained from the expression for q_2/b (equation (35)), and (38), is:

$$b^2 = \gamma \frac{y_1 + q_r y_2}{(y_1 y_2)^2}. \tag{40}$$

The above results are illustrated in figure 7 for an exchange flow with $q_r = 5$ and $b = \exp(x^2)$. A plan of the constriction is given in figure 7(*a*), and an elevation showing the variation of interface height in figure 7(*b*). The three heights y_{2v}, y_{20}, and y_{2m} are plotted showing that the virtual control and the point of marginal stability occur on opposite sides of the constriction. The virtual control is on the side where the slower moving layer is thinner.

The variations of F_Δ^2, G^2, and F_I^2 plotted in figure 7(*c*) satisfy the fundamental relationship for Boussinesq flows with negligible free-surface deflection (equation (24)). To the left of the virtual control the flow is supercritical with a passive upper layer. Between the virtual control and the throat the flow is subcritical. Note that the internal Froude number drops to zero at the point where the internal convective

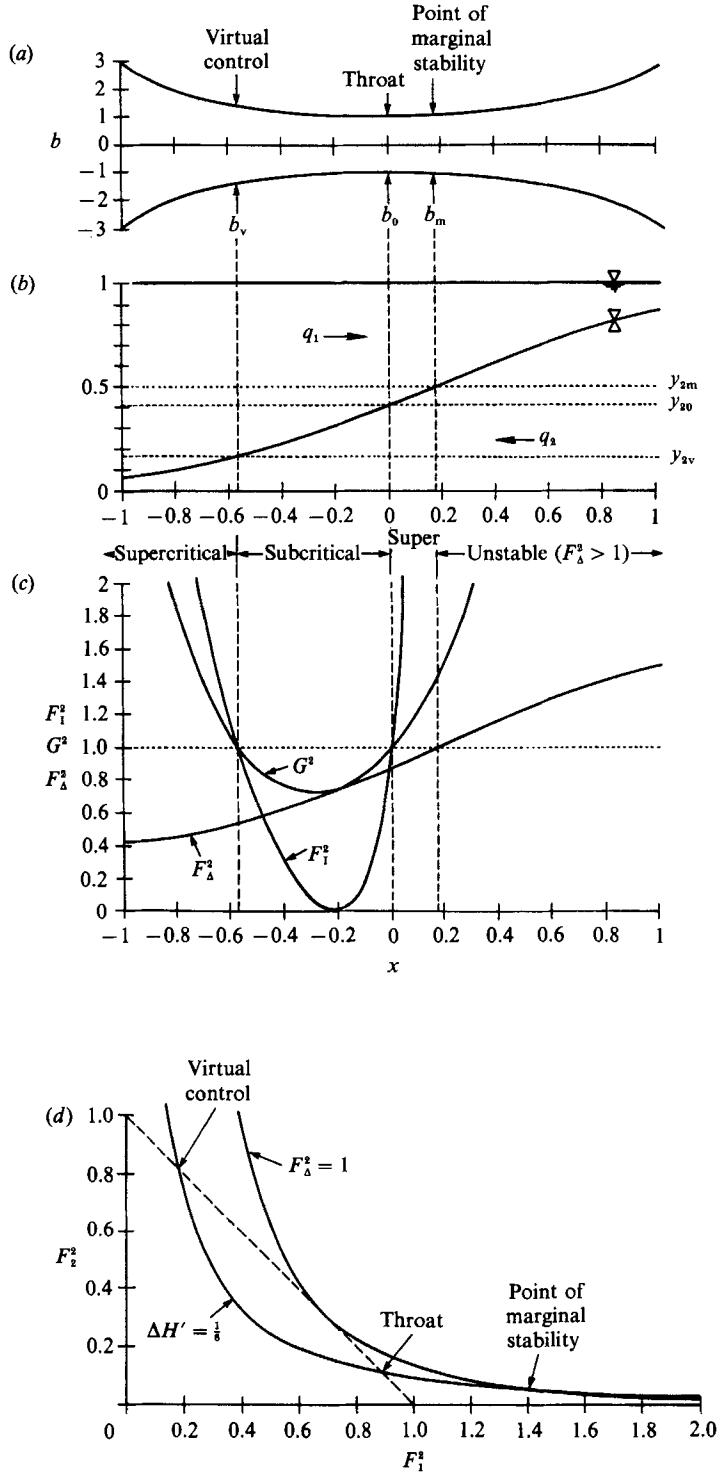

FIGURE 7. Boussinesq exchange flow through a contraction with $q_r = 5$ and $b = \exp(x^2)$. (*a*) Plan view of the constriction. (*b*) Plot of the variation of interface height. (*c*) Plot of the variations of F_1^2, F_Δ^2 and G^2. (*d*) Representation of the flow on the Froude number plane. The flow follows the line of constant dimensionless energy difference between the layers, $\Delta H = 1/(1+q_r) = \frac{1}{6}$.

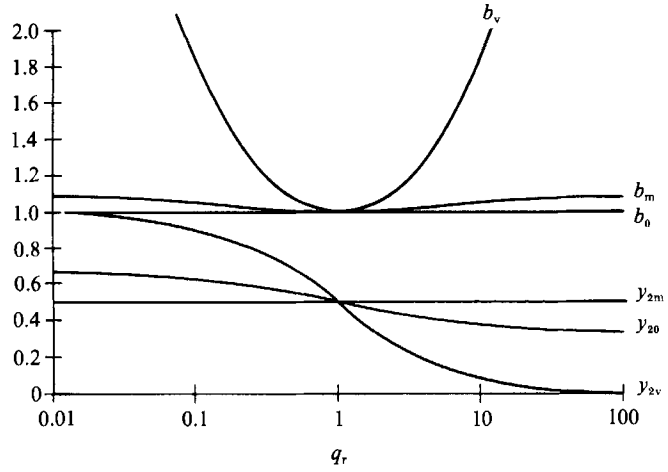

FIGURE 8. Plot of the variation with q_r of the widths and interface heights at the virtual control, the point of marginal stability, and the throat.

velocity, see (19*b*), equals zero, which for $q_r = 5$ corresponds to $y_2 = 1/(1+\sqrt{5})$. To the left of this point the internal convective velocity is negative, and to the right it is positive. Between the throat and the point of marginal stability the flow is internally supercritical. To the right of the point of marginal stability Long's stability criterion is violated and the validity of hydraulic analysis in this region must be questioned. In this region $F_I^2 < 0$, corresponding to imaginary convective velocities. Some of the above features are also represented on the Froude number plane given in figure 7(*d*).

Substituting y_{2v} and y_{2m} into equation (40) gives expressions for the width at the virtual control and at the point of marginal stability; i.e.:

$$b_v^2 \approx 2\gamma \frac{(1+q_r)^3}{q_r}, \tag{41a}$$

$$b_m^2 \approx 8\gamma(1+q_r). \tag{41b}$$

These variations are plotted on figure 8 together with the variations of y_{2v}, y_{20}, and y_{2m}. The most important new result is the fact that $b_m \leqslant b_v$ which ensures the presence of a region of unstable flow unless the constriction is highly asymmetric. For very large and very small values of q_r the width at the virtual control approaches infinity whereas the width at the point of marginal stability approaches a finite value:

$$(b_m)_{max} \approx (\tfrac{32}{27})^{\frac{1}{2}}. \tag{42}$$

So the width of the contraction at the point of marginal stability is always less than 9% greater than the width at the throat. Therefore significant regions of unstable flow can be expected in exchange flow through contractions.

4.2. *Non-Boussinesq maximal exchange flows*

The same procedure used in the analysis of Boussinesq flows is followed in the analysis of non-Boussinesq flows. However, simple algebraic solutions, such as those given above do not generally exist for non-Boussinesq flows. Figure 9 corresponds to the flow given in figure 7 except that $\epsilon = 0.5$. Two flows are qualitatively the same. There is a topographic control at the throat, an upstream virtual control, and a point of marginal stability downstream of the throat. The non-Boussinesq flow differs in

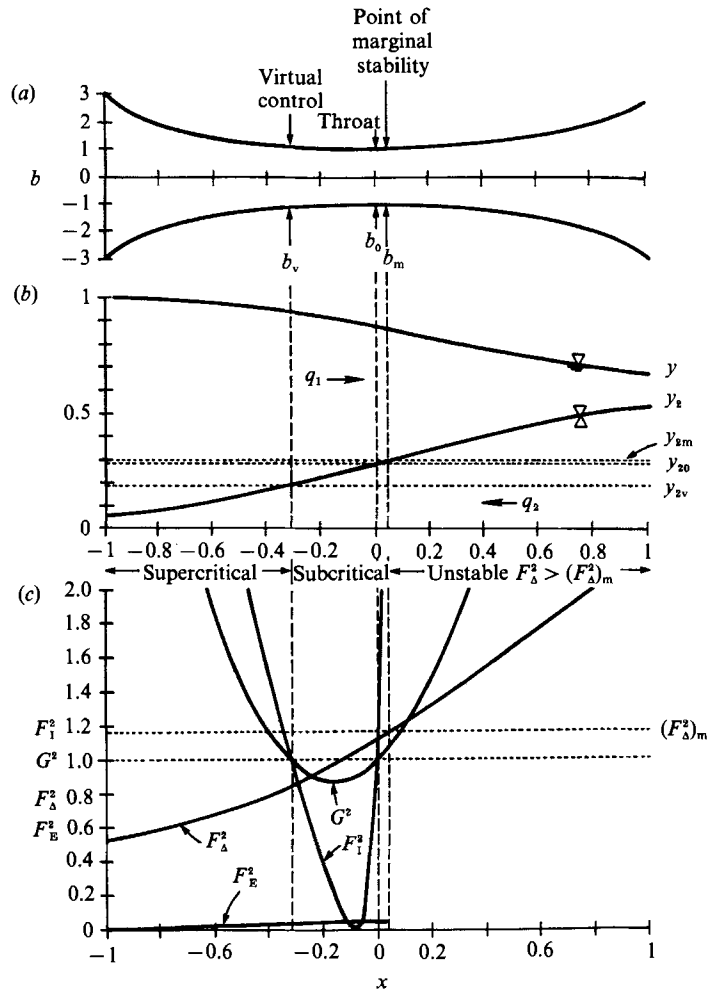

FIGURE 9. Non-Boussinesq exchange flow through a contraction with $\epsilon = 0.5$, $q_r = 5$ and $b = \exp(x^2)$. (*a*) Plan view of the constriction. (*b*) Plot of the variation of interface height. (*c*) Plot of the variations of F_I^2, F_Δ^2 and G^2.

that the free surface drops as the upper layer accelerates, the points of virtual control and marginal stability are closer to the throat, and the shear Froude number at the point of marginal stability $(F_\Delta^2)_m > 1$, in accordance with the results presented in figure 2. Further calculations show that as ϵ increases the virtual control continues to move downstream and eventually passes through the throat. The point of marginal stability remains to the right of the virtual control.

It is of most interest to consider the situation where the virtual and topographic controls coincide at the throat. In this case, the flow at the throat must satisfy the regularity condition (9), the Bernoulli equation for the upper layer (28), and it must be internally critical. The solution is remarkably simple; i.e. at the throat $F_1^2 = F_2^2$, which leads to a series of useful results. Firstly the two controls will coincide if, and only if,

$$q_r = (1-\epsilon)^{-\frac{3}{4}}. \tag{43}$$

This result is not surprising if we consider that as ϵ increases the ratio of the kinetic energy of the upper layer to that of the lower layer decreases, so that a higher q_r is

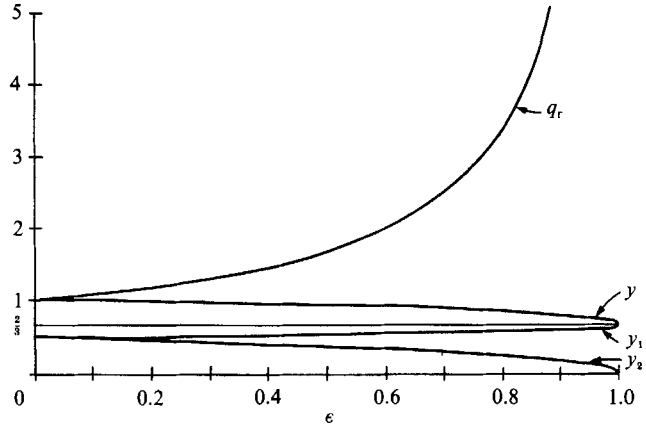

FIGURE 10. The variation with ϵ of q_r, y, y_1, and y_2 at the throat in flows where the two controls coincide.

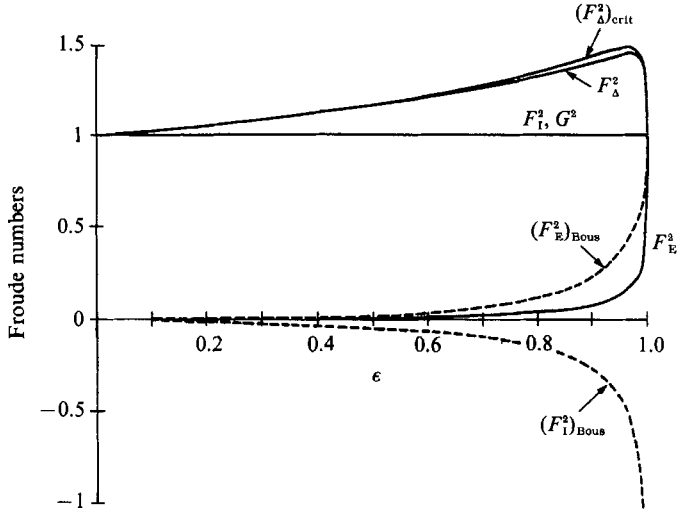

FIGURE 11. The variation with ϵ of the exact values F^2_E, F^2_I, F^2_Δ, $(F^2_\Delta)_{crit}$, and G^2, together with the Boussinesq approximations to F^2_E and F^2_I, at the throat in flows where the two controls coincide.

required to keep the virtual control in the same position. The variation of q_r, and of y_1, y_2, and y at the throat are plotted in figure 10. The layer thicknesses at the throat are given by:

$$y_1 = \frac{2}{3+(1-\epsilon)^{\frac{1}{2}}}, \tag{44a}$$

$$y_2 = \frac{2(1-\epsilon)^{\frac{1}{2}}}{3+(1-\epsilon)^{\frac{1}{2}}}. \tag{44b}$$

As $\epsilon \to 1$ the lower-layer thickness $y_2 \to 0, y_1 \to \frac{2}{3}$, and the flow behaves as if it were single layered, as we would expect from a comparison of the general matrix representations of single and two-layer flow (2) and (3).

The variations in the exact values of F^2_E and F^2_I when the two controls coincide are plotted in figure 11. The Boussinesq approximation for F^2_E, given by (21), behaves as

we would expect; it begins to diverge from the exact value as ϵ increases. However, the Boussinesq approximation for F_{I}^2, given by (20), always gives negative values, even though the exact (non-Boussinesq) solution is $F_{\mathrm{I}}^2 = 1$ for all values of ϵ. So irrespective of the value of ϵ we need to use the non-Boussinesq solutions. This result is explainable in terms of the variation of F_Δ^2 and $(F_\Delta^2)_{\mathrm{crit}}$. If $0 < \epsilon < 1$, then $1 < F_\Delta^2 < (F_\Delta^2)_{\mathrm{crit}}$, so although the flow is stable, the Boussinesq approximation for F_{I}^2 (equation (20*b*)) gives negative values, corresponding to an unstable flow.

4.3. *Discussion*

To fully appreciate the above results it must be remembered that Long's criterion is based on the assumption of a hydrostatic pressure distribution. Long (1956), himself, notes: 'If we abandon the hydrostatic assumption momentarily, we find that sufficiently short infinitesimal waves are unstable for any shear.' Even at values of $F_\Delta^2 \ll 1$ the interface is unstable to a number of short-wave instabilities (Thorpe 1987), the most notable being the Kelvin–Helmholtz instability. If the initial thickness of the density interface is sufficiently small, Kelvin–Helmholtz billows will form on the interface. These billows may become unstable to a subharmonic wave that causes alternate billows to pair. As this pairing proceeds smaller scale three-dimensional instabilities result in mixing at a molecular level. Pairing will continue until the billows becomes so large that the shear is no longer strong enough to overcome the buoyancy forces resisting pairing. At this stage Koop & Browand (1979) observed a collapse of the mixing layer leaving a density interface of thickness

$$\delta = J_{\mathrm{crit}} F_\Delta^2 h, \tag{45}$$

where the critical bulk Richardson number, $J_{\mathrm{crit}} = g'\delta/\Delta u^2$. The value of J_{crit} is about 0.3, but may depend on a number of factors including: the definition of δ; the shape of the velocity and density profiles; and the Reynolds and Prandtl numbers. This result is supported by the theoretical work of Miles (1961), Howard (1961) and Corcos & Sherman (1976); the numerical work of Hazel (1972); and experimental work of Thorpe (1973) and Lawrence (1985).

The thickness of the density interface given by (45) cannot be attained unless the flow is sufficiently deep. The constraining effect of the depth on the stability of a stratified shear flow has been investigated numerically by Hazel (1972). He solved the Taylor–Goldstein equation for the case of 'tanh' velocity and density profiles; i.e. assuming $u = \frac{1}{2}(u_1+u_2)+\frac{1}{2}\Delta u \tanh(2z/\delta)$, and $\rho = \frac{1}{2}(\rho_1+\rho_2)+\frac{1}{2}\Delta\rho \tanh(2z/\delta)$, where $-\frac{1}{2}h < z < \frac{1}{2}h$, and the 'vorticity' thickness $\delta = \Delta u/(\mathrm{d}u/\mathrm{d}z)_{\max}$. Data from figure 3 of Hazel (1972) has been used to plot figure 12. When $\delta/h = 0$, $(F_\Delta^2)_{\mathrm{crit}} = 1$, in accordance with Long's (1956) stability criterion, but $(F_\Delta^2)_{\mathrm{crit}}$ increases as δ/h increases.

Errors introduced into the hydraulic analysis owing to the presence of an interface of finite thickness may be reduced by the introduction of integral correction factors similar to those used in the hydraulic analysis of single-layer flows, see Wood (1970). The question that arises is now large a value of δ/h can be accommodated within the framework of hydraulic analysis? Hazel (1972) notes that the flow ceases to resemble a two-layer system when δ/h is about 0.37, tending towards a flow with uniform shear and linear density. This is close to the point $(\delta/h \approx 0.4; F_\Delta^2 \approx 1.6)$, that, according to figure 12, long waves become the most unstable waves. Thus, from two perspectives we cannot expect hydraulic analysis to accurately model the flow considered by Hazel (1972) when $F_\Delta^2 > 1.6$.

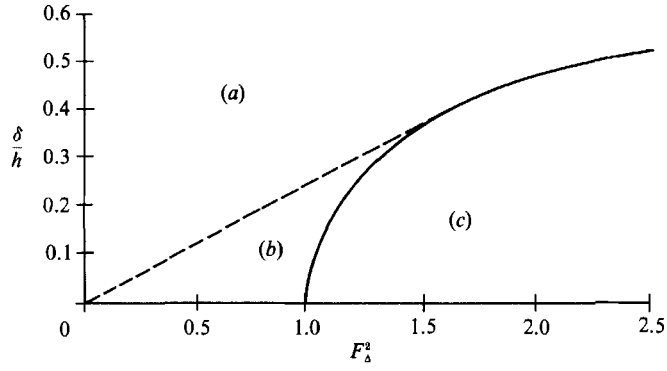

FIGURE 12. Stability diagram for flows with tanh velocity and density profiles. Computed from (Hazel 1972, figure 3). (*a*) All wavelengths are stable; (*b*) long waves are stable, but some short waves are unstable; and (*c*) long waves are unstable, and some short waves are unstable. – – – –, envelope of stability curves for waves of finite length, corresponding to $J_{\text{crit}} = 0.25$; ——, stability boundary for long waves.

This restriction still does not preclude the possibility of modelling exchange flows entirely; since, although F_Δ^2 may approach a value of 2, this only occurs when one layer is considerably thinner than the other, see figure 6. Figure 12 only applies for the case of equal layer thicknesses. Further results of Hazel (1972, figure 10) indicate that asymmetric flows are more stable than symmetric flows. In addition, Hazel showed that an unbounded flow with 'error function' profiles of velocity and density (as recommended by Scotti & Corcos 1972), was more stable than an unbounded flow with tanh profiles. So, it is still an open question as to whether hydraulic analysis can be used to effectively model exchange flow through a contraction.

5. Conclusions

The internal, external, stability, and composite Froude numbers are all of particular importance in the hydraulic analysis of both Boussinesq and non-Boussinesq two-layer flows. They are interrelated by the equation:

$$(1-G^2) = k(1-F_{\text{E}}^2)(1-F_{\text{I}}^2), \tag{23}$$

where $k \approx 1-F_\Delta^2$. This equation facilitates a comprehensive understanding of the hydraulics of both Boussinesq and non-Boussinesq two-layer flows.

If F_Δ^2 exceeds a critical value, which depends on the relative density difference between the layers, then Long's (1956) criterion for the stability of long waves is violated. Care must be taken when using the composite Froude number, since it cannot identify flows that violate Long's criterion. Both Boussinesq and non-Boussinesq exchange flows through a contraction violate Long's criterion. However, the presence of velocity and density interfaces of finite thickness, owing to the action of Kelvin–Helmholtz instabilities, and in violation of the hydraulic assumptions, may render exchange flows stable to long waves. It is not yet known whether hydraulic analysis can be modified to accurately model flows with interfaces of finite thickness. This problem provides a worthwhile challenge, since it could aid in the prediction of mixing in many stratified shear flows.

I wish to acknowledge the support of the Departments of Civil Engineering at the University of British Columbia and the University of California, at Berkeley. Partial funding was provided by the Canadian Natural Sciences and Engineering Research Council, and the US National Science Foundation. I am deeply grateful to Gilles Corcos and the late Hugo Fischer for providing the inspiration to pursue this study; and to Larry Armi, Fred Browand, Richard Denton, Liam Finn, Stephen Monismith, Harry Yeh, Emily Cheung, and Takis Labridis for their valuable comments on earlier drafts of this paper.

Appendix. Exact derivation of the characteristic velocities of long waves

The characteristic velocities (celerities), λ, of both long internal and long external waves are specified by the eigenvalue equation (4):

$$\mathrm{Det}\,(\boldsymbol{C}-\lambda\boldsymbol{I}) = 0, \tag{A 1}$$

where $\boldsymbol{I}$ is the identity matrix. Substituting for the matrix $\boldsymbol{C}$ given in (3) yields:

$$\sum_{m=0}^{4} a_m \lambda^m = 0, \tag{A 2}$$

where
$$a_0 = u_1^2 u_2^2 - g h_1 u_2^2 - g h_2 u_1^2 + g g' h_1 h_2 = g g' h_1 h_2 (1-G^2),$$
$$a_1 = -4 u_1 u_2 \bar{u} + 2 g h \hat{u},$$
$$a_2 = 4\bar{u}^2 + 2 u_1 u_2 - g h,$$
$$a_3 = -4\bar{u},$$
$$a_4 = 1,$$

and
$$\bar{u} = \tfrac{1}{2}(u_1+u_2), \quad \hat{u} = (u_1 h_2 + u_2 h_1)/h, \quad \text{with } h = h_1 + h_2.$$

General solutions for quartic equations are given in many mathematical handbooks; the Descartes–Euler solution, see Korn & Korn (1968, p. 24), is used here. The first step is the substitution of $\lambda = y + \bar{u}$ into the quartic equation (A 2) to obtain the reduced quartic equation:

$$y^4 + d y^2 + e y + f = 0, \tag{A 3}$$

where $d = \frac{1}{2} g h (2 + \epsilon F_\Delta^2)$, $e = 2 g h (\hat{u} - \bar{u})$, $f = (\frac{1}{4} g h)^2 \{4\epsilon(\alpha - F_\Delta^2) + \epsilon^2 F_\Delta^4\}$, and $\alpha = 4 h_1 h_2 / h^2$. Note that if $u_1 = u_2$, then $d = -gh$, $e = 0$, and $f = 4\epsilon\alpha(\frac{1}{4} g h)^2$, giving the equation solved by Stokes (1847, see Gill 1982, p. 121). The solutions are:

$$\lambda_{\mathrm{E}}^{\pm} = \bar{u} \pm (\tfrac{1}{2} g h (1 + (1 - \epsilon\alpha)^{\frac{1}{2}}))^{\frac{1}{2}}, \tag{A 4a}$$

$$\lambda_{\mathrm{I}}^{\pm} = \bar{u} \pm (\tfrac{1}{2} g h (1 - (1 - \epsilon\alpha)^{\frac{1}{2}}))^{\frac{1}{2}}. \tag{A 4b}$$

These solutions are real since $\alpha\epsilon < 1$. If $\alpha\epsilon \ll 1$, then $c_{\mathrm{E}} \approx (gh)^{\frac{1}{2}}$ and $c_{\mathrm{I}} \approx (g' h_1 h_2 / h)^{\frac{1}{2}}$.

If $u_1 \neq u_2$ the four solutions of the reduced quartic equation (A 3) are:

$$y_1 = \zeta z_1^{\frac{1}{2}} + z_2^{\frac{1}{2}} + z_3^{\frac{1}{2}}, \tag{A 5a}$$

$$y_2 = -\zeta z_1^{\frac{1}{2}} - z_2^{\frac{1}{2}} + z_3^{\frac{1}{2}}, \tag{A 5b}$$

$$y_3 = -\zeta z_1^{\frac{1}{2}} + z_2^{\frac{1}{2}} - z_3^{\frac{1}{2}}, \tag{A 5c}$$

$$y_4 = \zeta z_1^{\frac{1}{2}} - z_2^{\frac{1}{2}} - z_3^{\frac{1}{2}}, \tag{A 5d}$$

where $\zeta = \mathrm{sgn}\,(u_2 - u_1)$, and z_1, z_2, z_3 are the solutions of the normalized cubic resolvent of (A 3):

$$z^3 + rz^2 + sz + t = 0, \tag{A 6}$$

where

$$r = -\tfrac{1}{2}\mathrm{i} = -(\tfrac{1}{40}gh)\,(2 + \epsilon F_\Delta^2),$$

$$s = \tfrac{1}{16}(\mathrm{i}^2 - 4k) = (\tfrac{1}{40}gh)^2\{1 + \epsilon(2F_\Delta^2 - \alpha)\},$$

and

$$t = -\tfrac{1}{64}\mathrm{j}^2 = -\epsilon(\tfrac{1}{40}gh)^3(1-\alpha)\,F_\Delta^2.$$

The solutions of the normalized cubic resolvent (A 6) depend on the value of its discriminant

$$D = (\tfrac{1}{3}p)^3 + (\tfrac{1}{2}q)^2, \tag{A 7}$$

where $p = \frac{1}{3}(3s - r^2)$ and $q = \frac{1}{27}(2r^3 - 9rs + 27t)$. The algebraic programming system REDUCE was used to determine that:

$$D = -\frac{\alpha\epsilon(\frac{1}{40}gh)^6}{108}\left\{\beta + (1 - F_\Delta^2)\sum_{n=0}^{3} b_n\,\epsilon^n\right\}, \tag{A 8}$$

where

$$b_0 = 4,$$

$$b_1 = (27\alpha - 12)\,F_\Delta^2 - 9\alpha,$$

$$b_2 = 12F_\Delta^4 - 18\alpha F_\Delta^2,$$

$$b_3 = -4F_\Delta^6,$$

$$\beta = \alpha\epsilon\{1 + 2\epsilon(2\alpha - F_\Delta^2) + \epsilon^2 F_\Delta^4\}.$$

The value of D is dependent on the values of the three parameters, α, ϵ, and F_Δ^2. From basic physical considerations $0 < \epsilon < 1, 0 < \alpha \leqslant 1$, and $F_\Delta^2 \geqslant 0$. The requirement that $D \leqslant 0$ for the solutions to be real restricts the value of F_Δ^2 to be less than or equal to a critical value $(F_\Delta^2)_{\mathrm{crit}}$. The variation of $(F_\Delta^2)_{\mathrm{crit}}$ with ϵ for $\alpha = 0.25$, 0.5, and 1.0 is plotted in figure 2.

If $D \leqslant 0$, then the roots of the normalized cubic resolvent (A 6) are:

$$z_n = 2\gamma\cos(\tfrac{1}{3}\phi + \tfrac{2}{3}n\pi) - \tfrac{1}{3}r \quad (n = 1, 3), \tag{A 9}$$

where

$$\gamma = \left(-\frac{p}{3}\right)^{\frac{1}{2}}, \quad \cos\phi = -\frac{q}{2\gamma^3}, \quad \sin\phi = \frac{(-D)^{\frac{1}{2}}}{\gamma^3},$$

$$p = -\frac{(\frac{1}{40}gh)^2}{3}\{1 + \epsilon(3\alpha - 2F_\Delta^2) + \epsilon^2 F_\Delta^4\}$$

and

$$q = \frac{(\frac{1}{40}gh)^3}{27}\{2 + \epsilon(27\alpha F_\Delta^2 - 18\alpha - 6F_\Delta^2) + \epsilon^2(6F_\Delta^4 - 9\alpha F_\Delta^2) - 2\epsilon^3 F_\Delta^6\}.$$

Finally, the exact solutions to the quartic equation (A 2) are:

$$\lambda_{\mathrm{E}}^{\pm} = \bar{u} + \zeta z_1^{\frac{1}{2}} \pm (z_3^{\frac{1}{2}} + z_2^{\frac{1}{2}}), \tag{A 10a}$$

$$\lambda_{\mathrm{I}}^{\pm} = \bar{u} - \zeta z_1^{\frac{1}{2}} \pm (z_3^{\frac{1}{2}} - z_2^{\frac{1}{2}}), \tag{A 10b}$$

where, $\zeta = \mathrm{sgn}\,(u_2 - u_1)$. A similar set of solutions has been obtained independently by Artale & Levi (1988) in their study of the propagation of solitary waves.

If $D > 0$, then z_1 is real, and z_2 and z_3 are complex conjugates, and the internal phase velocity, $z_3^{\frac{1}{2}} - z_2^{\frac{1}{2}}$, is imaginary, corresponding to the instability of long internal waves.

REFERENCES

ARMI, L. 1975 The internal hydraulics of two flowing layers of different densities. PhD thesis, University of California, Berkeley.

ARMI, L. 1986 The hydraulics of two flowing layers of different densities. *J. Fluid Mech.* **163**, 27.

ARMI, L. & FARMER, D. M. 1986 Maximal two-layer exchange flow through a contraction with barotropic net flow. *J. Fluid Mech.* **164**, 27.

ARMI, L. & FARMER, D. M. 1989 The flow of Mediterranean water through the Strait of Gibraltar. *Prog. Oceanogr.* **21**, 1.

ARTALE, V. & LEVI, D. 1988 Solitary waves in straits. In *Nonlinear Evolutions* (ed. J. J. Leon). World Scientific.

BAINES, P. G. 1984 A unified description of two-layer flow over topography. *J. Fluid Mech.* **146**, 127.

BAINES, P. G. 1988 A general method for determining upstream effects in stratified flow of finite depth over long two-dimensional obstacles. *J. Fluid Mech.* **188**, 1.

BENTON, G. S. 1954 The occurrence of critical flow and hydraulic jumps in a multilayered fluid system. *J. Met.* **11**, 139.

CORCOS, G. M. & SHERMAN, F. S. 1976 Vorticity concentration and the dynamics of unstable free shear layers. *J. Fluid Mech.* **73**, 241.

DENTON, R. A. 1987 Locating and identifying hydraulic controls for layered flow through an obstruction. *J. Hydraul. Res.* **25**, 281.

FARMER, D. M. & ARMI, L. 1986 Maximal two-layer exchange over a sill and through the combination of a sill and contraction with barotropic flow. *J. Fluid Mech.* **164**, 53.

FARMER, D. M. & ARMI, L. 1989 The flow of Atlantic water through the Strait of Gibraltar. *Prog. Oceanogr.* **21**, 1.

GILL, A. E. 1982 *Atmosphere–Ocean Dynamics.* Academic.

HAZEL, P. 1972 Numerical studies of the stability of inviscid stratified shear flows. *J. Fluid Mech.* **51**, 39.

HENDERSON, F. M. 1966 *Open Channel Flow.* Macmillan.

HOUGHTON, D. D. & ISAACSON, E. 1970 Mountain winds. *Stud. Num. Anal.* **2**, 21.

HOWARD, L. N. 1961 Note on a paper of John W. Miles. *J. Fluid Mech.* **10**, 509.

KOOP, C. G. & BROWAND, F. K. 1979 Instability and turbulence in a stratified fluid with shear. *J. Fluid Mech.* **93**, 135.

KORN, G. A. & KORN, T. M. 1968 *Mathematical Handbook for Scientists and Engineers: Definitions, Theorems, and Formulas for Reference and Review.* McGraw-Hill.

LAWRENCE, G. A. 1985 The hydraulics and mixing of two-layer flow over an obstacle. PhD thesis, University of California, Berkeley.

LAWRENCE, G. A. 1987 Steady flow over an obstacle. *J. Hydraul. Engng* **113**, 981.

LONG, R. R. 1954 Some aspects of the flow of stratified fluids. II. Experiments with a two-fluid system. *Tellus* **6**, 97.

LONG, R. R. 1956 Long waves in a two-fluid system. *J. Met.* **13**, 70.

MILES, J. W. 1961 On the stability of heterogeneous shear flows. *J. Fluid Mech.* **10**, 496.

PRANDTL, L. 1952 *Essentials of Fluid Dynamics.* Blackie & Sons.

SCHIJF, J. B. & SCHÖNFELD, J. C. 1953 Theoretical considerations on the motion of salt and fresh water. In *Proc. of the Minn. Intl Hyd. Conv. Joint meeting of the IAHR and Hyd. Div. ASCE*, p. 321.

SCOTTI, R. S. & CORCOS, G. M. 1972 An experiment on the stability of small disturbances in a stratified free shear flow. *J. Fluid Mech.* **52**, 499.

STOKES, G. G. 1847 On the theory of oscillatory waves. *Trans. Camb. Phil. Soc.* **8**, 441.

STOMMEL, H. & FARMER, H. G. 1953 Control of salinity in an estuary by a transition. *J. Mar. Res.* **12**, 13.

THORPE, S. A. 1973 Experiments on instability and turbulence in a stratified shear flow. *J. Fluid Mech.* **61**, 731.

THORPE, S. A. 1987 Transitional phenomena of turbulence in stratified fluids. *J. Geophys. Res.* **92**, 5231.

TURNER, J. S. 1973 *Buoyancy Effects in Fluids.* Cambridge University Press.

WOOD, I. R. 1968 Selective withdrawal from a stably stratified fluid. *J. Fluid Mech.* **32**, 209.

WOOD, I. R. 1970 A lock exchange flow. *J. Fluid Mech.* **42**, 671.